JMEPEG (2005) 14:91-98
DOI: 10.1361/10599490522176

1059-9495/$19.00

Prediction of Crack Deflection in Titanium Alloys with a Platelet Microstructure

N.L. Richards

(Submitted March 9, 2004)

Comparison has been made of the crack path through a conventional solution heat-treated and aged microstructure in two titanium alloys with that of a double-heat-treated microstructure containing α platelets. Crack-opening displacement calculations from theory developed in the literature were used to predict the crack path based on deflection past the platelets, or cutting through the α platelets, based on the minimization of energy needed for the crack to propagate through the microstructure.

Keywords crack-opening displacement, crack path, fracture toughness, microstructure, titanium alloys

1. Introduction

Beta forging has been used by the titanium industry since the 1960s to increase the fracture toughness of α-β titanium (Ti) alloys relative to forging below the β transus. Coyne (Ref 1), for example, reported an increase in fracture toughness values for alloy Ti-6Al-4V from 44 to 55 MN/m$^{3/2}$ to 66 to 77 MN/m$^{3/2}$, without any reduction in tensile strength, though reduction in area values dropped from 38 to 25%. In addition, several authors (Ref 2-5) have investigated the influence of grain shape change from equiaxed to acicular, with the general trend showing an increase in fracture toughness accompanied by a reduction in tensile ductility. Fentiman et al. (Ref 6) investigated the effect on fracture toughness in a Ti-11Sn-2.25Al-4Mo-0.2Si α-β alloy, in which the acicular structure had higher toughness than the equiaxed one at strength levels up to 1240 MN/m^2. With a similar microstructure in a Ti-6Al-6V alloy (Ref 7), a toughness increase of 40% was achieved with only a 5% reduction in strength. Margolin and Greenfield (Ref 8) showed that the change in ΔK_q for a Ti-5.25Al-5.5V-0.9Fe-0.5Cu alloy was related to the thickness of the β grain boundary α of β-processed material.

Eylon et al. (Ref 9) investigated a forged near α Ti-11 alloy, above and below the β transus that showed a 70% increase in toughness with no effect on the tensile properties in the water-quenched condition. A previous article (Ref 10) discussed the behavior of Ti using a combination of forging above and below the β transus on two Ti alloys, combined with solution heat treatment also above and below the β transus. The heat treatment was referred to as a double heat treatment (DHT) and resulted in increased levels of fracture toughness in both alloys, one by 100% (alloy A) and the other by 25% (alloy B). On average, strength parameters were reduced by about 5%, with ductility values being 50 to 75% of the conventionally solution heat-treated and aged alloy. Thus, it can be seen that β forging is beneficial to fracture toughness values, as well as improved forgeabilty in practice, combined with shorter fabrication cycles and closer tolerances (Ref 11).

The present article is concerned with a quantitative analysis of the potential of the α platelets to deflect, or not deflect, a propagating crack and, as a consequence, will attempt to explain the reason for the DHT microstructure to show higher fracture toughness values compared with the conventional equiaxed microstructure.

1.1 Development of Analysis Methodology

By influencing the morphology of the microstructure of the two alloys via forging and heat treatment, the percentage of α and β, as well as their shape, can be varied. The α phase, for example, is softer than the β phase and, thus, is tougher. Varying the thickness of the α phase by thermomechanical processing also influences the crack propagation behavior of the alloys.

Goodier and Field (Ref 12) have analyzed the crack tip displacement and shown that the critical crack-opening displacement (COD), δ_c, at the elastic-plastic boundary can be estimated by:

$$\delta_c = \frac{8\sigma_{ys}c}{\pi E} \ln\left(\frac{\sec\pi\sigma}{2\sigma_{ys}}\right) \quad \text{(Eq 1)}$$

In this equation, E is Young's modulus, c is the half crack length, σ is the nominal stress, and σ_{ys} is the material yield stress. At low values of T/σ_{ys} (<0.6), Eq 1 can be reduced to:

$$\delta_c = \frac{\Pi K^2}{2E\sigma_{ys}} \quad \text{(Eq 2)}$$

where K is stress intensity factor. Wells (Ref 13) has also developed an expression for δ_c as:

$$\delta_c = \frac{4K_1^2}{\Pi\sigma_{ys}} \quad \text{(Eq 3)}$$

N.L. Richards, Department of Mechanical & Manufacturing Engineering, University of Manitoba, Winnipeg, MB, Canada R3T 5V6. Contact e-mail: nrichar@cc.umanitoba.ca.

with K_1 indicating the opening mode. Under plane strain conditions, this equation can be written as:

$$\delta_c = \frac{4K_{1c}^2 (0.61)}{\Pi\sigma_{ys}} \quad \text{(Eq 4)}$$

The 0.61 factor is a correction term for a plane strain von Mises material (Ref 14). In the present analysis, use will be made of the equation of Wells (Ref 13), with the only difference being in the numerical values between the two equations.

At a point ahead of the crack tip, Hahn and Rosenfield (Ref 15), following Goodier and Field (Ref 12), give the displacement δ_x as:

$$\delta_x = \frac{(k+1)\, c\sigma_{ys}}{8\pi G} + \cos\theta \log\frac{\sin^2(\theta_2 - \theta)}{\sin^2(\theta_2 + \theta)} + \cos\theta_2 \log\frac{(\sin\theta_2 + \sin\theta)^2}{(\sin\theta_2 - \sin\theta)^2} \quad \text{(Eq 5)}$$

In Eq 5, G is the shear modulus, σ_{ys} is the yield stress in the plastic zone, k is equal to $[(3 - \upsilon)/(1 + \upsilon)]$ for plane stress conditions and (3 to 4 υ) for plane strain conditions, θ is equal to the $\cos^{-1}(x/c)$, where c is the half crack length + $2r_y$ and r_y is the diameter of the plastic zone, and θ_2 is equal to the product $(\sigma/\sigma_{ys})(\pi/2)$.

Hahn and Rosenfield (Ref 15), from Eq 1, were able to determine a normalized displacement based on δ_x/δ_c. Gerberich and Baker (Ref 7) also used this approach to successfully predict crack deflection in a Ti-6Al-4V alloy having an acicular microstructure.

Using the equation of Wells (Ref 13) (Eq 4 from above) to predict δ_c, and the normalized displacement parameter of Hahn and Rosenfield (Ref 15), it is possible to predict the crack deflection behavior in the two alloys using the following sequence of calculations:

1. Calculate from the Wells equation, the appropriate δ_c value, using the fracture toughness data and mechanical properties evaluated in the experimental section.
2. From the Hahn and Rosenfield approach, evaluate ($\delta_{xDHT}/\delta_{cDHT}$) as ($\delta_{xDHT}/\delta_{cDHT} = L/2r_y$), and calculate δ_{xDHT}, the δ_x value being the length of the microstructural parameter L ahead of the crack tip. In a previous article (Ref 10), an average value for L was determined where a measure of the α platelet of 45° to the main axis of the crack was used.
3. Calculate δ_{cm}, the matrix δ_c value, from parameters determined in the experimental section.
4. Compare δ_{xDHT} with δ_{cm}. If $\delta_{xDHT} < \delta_{cm}$, then the crack will deflect past suitably inclined α platelets. Otherwise, if less energy is expended in cutting through the platelets, then the crack will propagate straight ahead and not deflect.

2. Experimental

The compositions of the two alloys are shown in Table 1. Both alloys were received as 10 cm square billets. Forging of the alloys was carried out from 950, 1050, and 1125 °C with forging reductions of about 70%. Blanks were cut from the forgings and were heat treated as follows for the DHT.

Table 1 Chemical composition of alloys, in weight percent

Alloy	Al	V	Fe	C	O	N
Alloy A	6.15	3.97 Zr	0.08 Mo	0.03 Cu	1800 ppm	82 ppm Si
Alloy B	6.0	5.0	4.0	1.0	1200 ppm	0.2

2.1 Alloy A

1(a): Cool from 1040 to 675 °C at 32 °C/h. Preliminary tests showed that cooling below 700 °C precipitated sufficient α platelets.
1(b): Solution heat treat at 800, 900, and 950 °C, air cool, and then age at 500 °C for 24 h.
2: As in 1(a) and then solution heat treat at 800, 850, and 900 °C, oil quench, and age.

2.2 Alloy B

Cool from 1020 to 675 °C at 32 °C/h. Solution heat treat at 800, 875, and 950 °C, water quench, and then age at 510 °C for 8 h.

The 32 °C/h controlled cooling rate was shown previously to produce the type of microstructure suitable for investigating the variation in volume fraction of phases with suitable α platelets for toughness-microstructural examination (Ref 10). Fracture toughness testing was carried out in accordance with ASTM E 399 using three-point bending specimens with a span-to-width ratio of 4 to 1. Three test samples were tested at each temperature, two to evaluate fracture toughness and one for microstructural examination of the plastic zone ahead of the crack.

Optical metallography was carried out using standard metallographic procedures with a final etch in Kroll's reagent (2% HF, 10%, HNO_3, 88% water). Accentuation of the transformed β phase was accomplished using 0.5% HF after the Kroll's reagent etch. Scanning electron microscopy (SEM) was used as the main metallographic technique. Quantitative metallographic parameters were measured automatically using image analysis.

Tensile testing on the solution heat-treated alloys was carried out using round tensile specimens and procedures outlined in ASTM E 8. Yield strength is reported as the 0.2% extension along with ultimate tensile strength and percentage elongation in 25 mm. Young's modulus was measured ultrasonically from measurement of the longitudinal and transverse wave velocities.

The volume fraction of voids in the plastic zone ahead of the tip on fracture test pieces was carried out manually by point counting on SEM micrographs. In alloy A, approximately 500 points were used to determine the void fraction, but, due to the increased toughness of alloy B relative to alloy A, measurement of a reasonable fraction of the voids in alloy B was not possible.

3. Results

Figure 1(a) to (d) shows the conventional solution heat-treated (SHT) and aged (SHT/A) and DHT and aged (DHT/A)

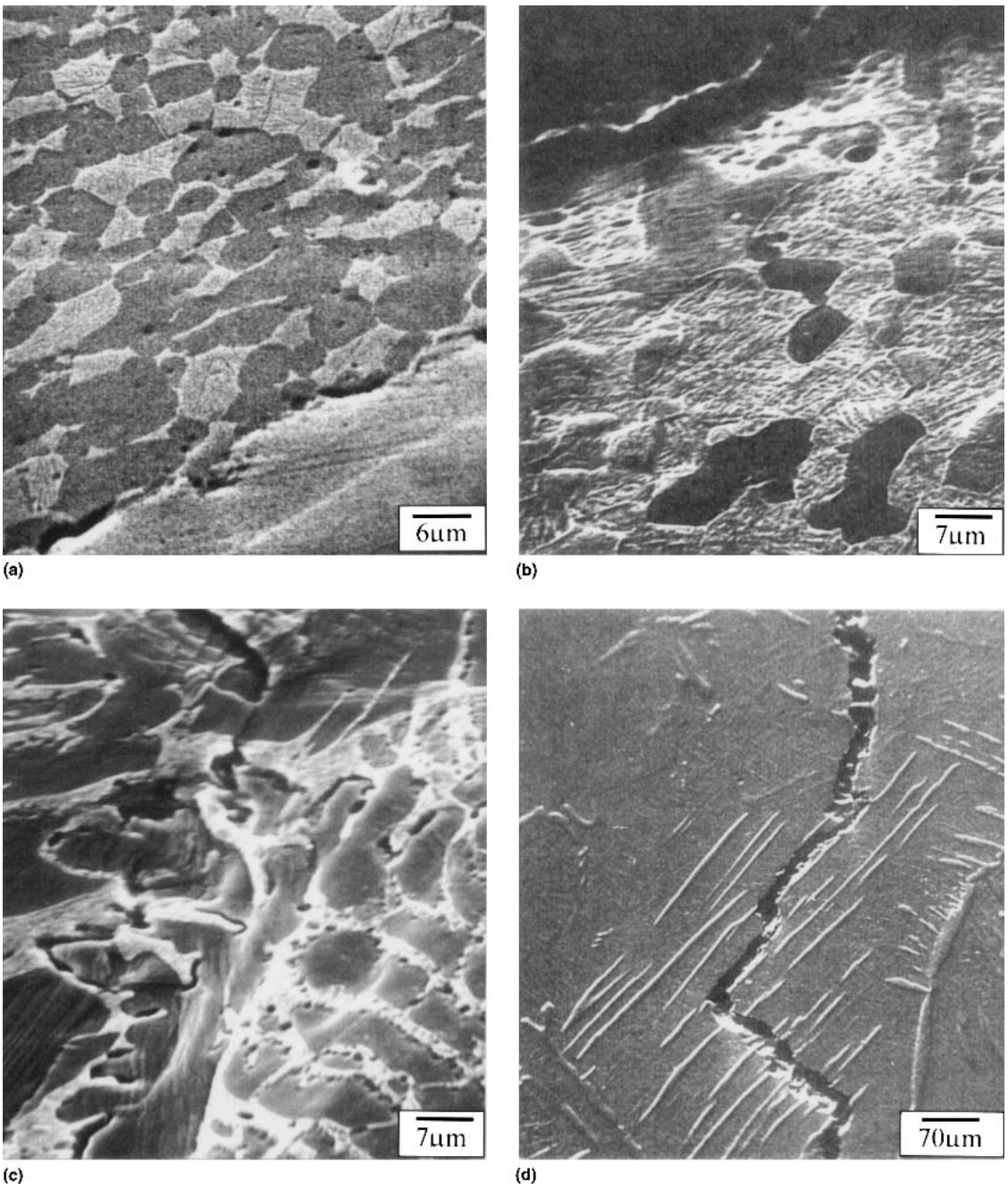

Fig. 1 SEM micrographs of microstructure and crack paths: alloys A and B. (a) STA microstructure and crack path: alloy A. (b) STA microstructure and crack path: alloy B. (c) Crack deviating around α platelets: alloy A. (d) Crack propagating through microstructure: alloy B

microstructures for both alloys A and B. In the SHT/A condition, alloy A (Fig. 1a) consists of equiaxed α (light) and the associated transformed β (dark). In the DHT condition (Fig. 1c), a composite type structure is formed with alternating α and transformed β phases, with the α phase exhibiting a platelet shape. The volume fraction and thickness of the α phase is determined by the prior processing history that is, whether it is α/β or β processed, and the subsequent solution heat treatment temperature. Prior β grain boundaries were covered with precipitated α, and, within the prior β grains, colonies of α and transformed β were observed to be inclined at various angles to each other. Within the colonies, the platelets were of similar orientation.

Alloy B in the SHT/A condition (Fig. 1b) consists of equiaxed α in a transformed β matrix. The DHT/A treatment of alloy B resulted in a similar microstructure to alloy A, with α platelets in a matrix of transformed β (Fig. 1d). Also shown in Fig. 1(c) and (d) are crack paths through the microstructure.

Figure 2 shows the fracture toughness-percent void relationship for void fractions adjacent to propagating cracks. The

relationship between fracture toughness and yield strength was expected to be an inverse relationship, and, as can be seen in Fig. 3(a) and (b), this occurred for both alloys. Graphs of K_{1c} versus α platelet thickness and interplatelet (β) spacing are shown in Fig. 4(a) to (d). As can be seen, the toughness increases directly with the α platelet thickness and inversely with the platelet spacing in both alloys. Young's modulus values for alloys A and B were measured as 117 and 110 GPa, respectively.

3.1 Quantitative Crack Deflection Analysis

Using the analysis developed earlier, and the data generated from these experiments, it is possible to examine the effects of the heat treatments on the passage of a crack through the microstructure. From Fig. 4, the size, volume fraction, and distribution of the α phase are seen to directly affect the fracture toughness of the alloys. Quantitatively, therefore, the α platelet size and spacing influence the toughness of the alloys, and, thus, the metallographic parameters should also influence crack direction as it propagates through the microstructure. Intuitively, one would expect the crack to take the path of least resistance, and thus, if a crack meets an α platelet of suitable thickness and inclination, it may be energetically favorable for the crack to deflect past the platelet, rather than cut it.

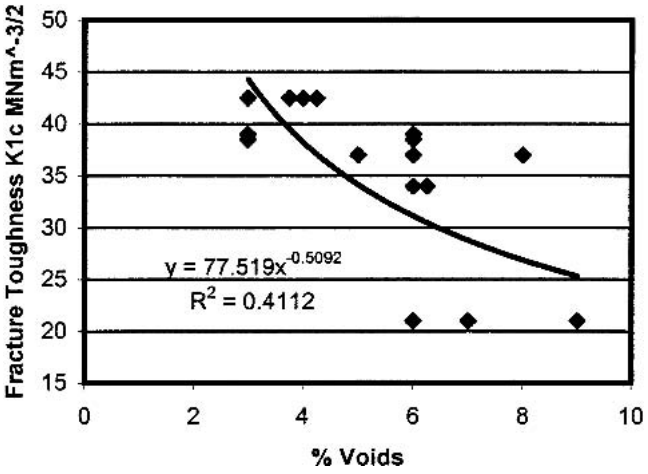

Fig. 2 Fracture toughness versus percentage of voids

3.2 Potential for Crack Deflection: Alloy A

Comparison can be made for a conventionally SHT/A material with a DHT/A alloy at the same solution heat treatment temperature. Table 2 shows heat treatment details, as well as the fracture toughness, yield strength, and microstructural parameters. For the SHT/A matrix (alloy A1) using Eq 4, and with δ_{cm} equal to the matrix COD:

$$\delta_{cm} = \frac{4K_{1c}^2\,(0.61)}{\Pi\sigma_{ys}} \qquad \text{(Eq 4)}$$

Using the parameters from Table 2, δ_{cm} is equal to 2.7 μm in plane strain. For alloy A in the DHT/A condition (alloy A2), and making a similar calculation, δ_{cDHT} is equal to 7.1 μm. From the analysis of Hahn and Rosenfield (Ref 15), if one equates the distance ahead of the crack tip to a microstructural parameter, as illustrated in Fig. 5, and then normalize the length L to the plastic zone size, then $\delta_{xDHT}/\delta_{cDHT}$ can be evaluated. The microstructural parameter that gave the best fit the experimental data for alloy A was $\sqrt{2}(\lambda_\alpha + \lambda_\beta)$.

The plastic zone diameter $2r_y$ was calculated from the equation of Irwin (Ref 16):

$$2r_y = \frac{1}{3\Pi}\left(\frac{K_{1c}}{\sigma_{ys}}\right)^2$$

From the quantitative microstructural analysis for alloy A2, the average λ_α value at 36 MPa$\sqrt{m}$ is 5.8 μm with λ_β equal to 3.1 μm. Consequently, $\sqrt{2}(\lambda_\alpha+\lambda_\beta)$ is equal to 12.6 μm. Thus, substituting these values into:

$$\frac{L}{2r_y} = \frac{\sqrt{2(\lambda_\alpha + \lambda_\beta)}}{2r_y}$$

yields a value of 0.13.

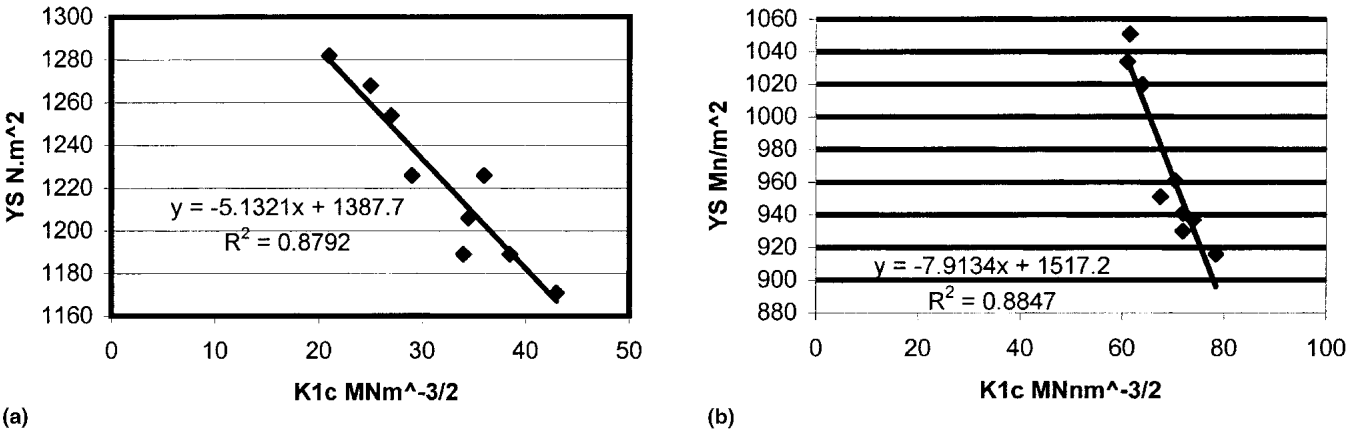

Fig. 3 Yield strength versus fracture toughness. (a) Alloy A. (b) Alloy B

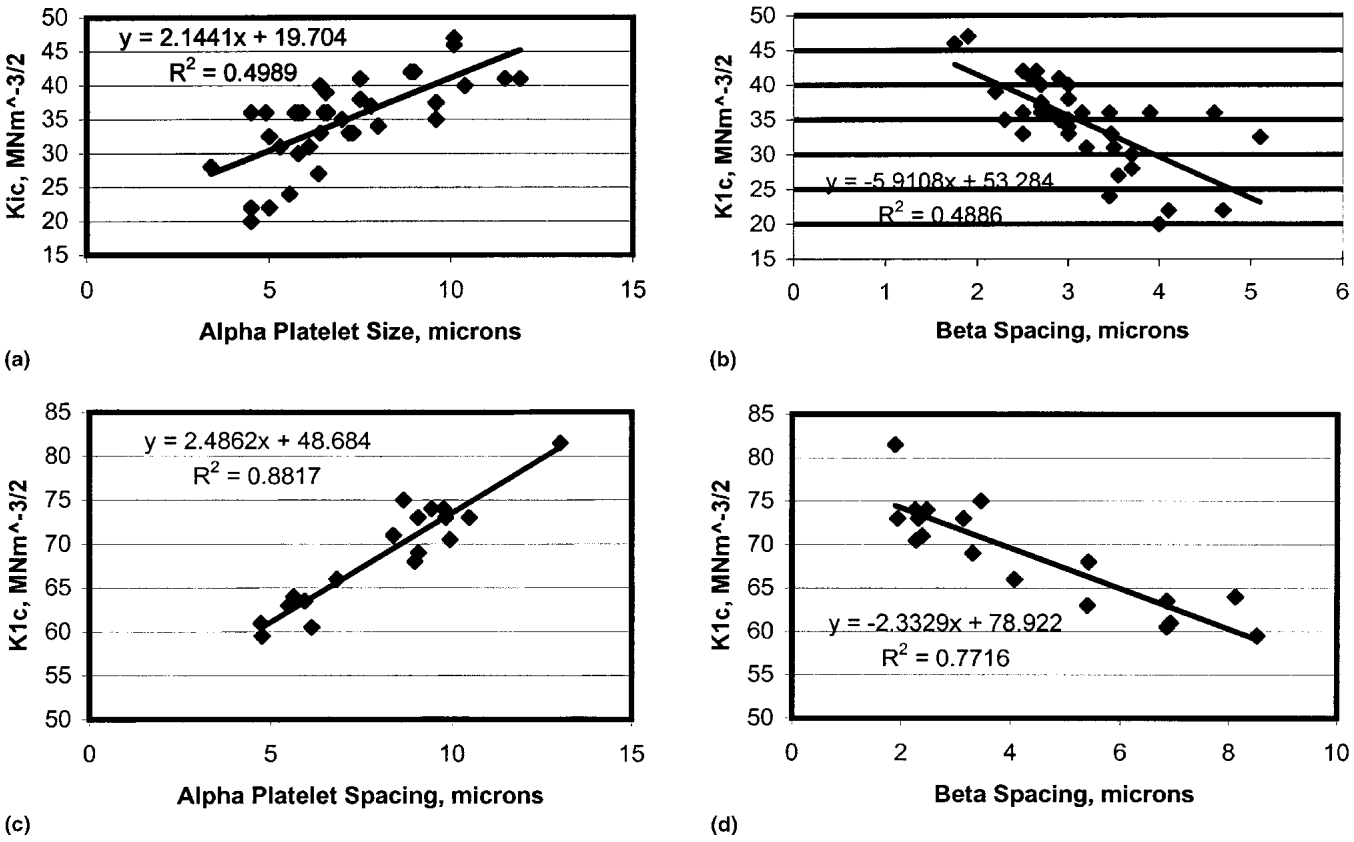

Fig. 4 Fracture toughness versus microstructural parameters. (a) and (b) Alloy A. (c) and (d) Alloy B

Table 2 Summary table for crack-opening displacement

Alloy	K_{1c} MPa$\sqrt{m}$	Heat treatment	Yield strength, MPa	λ_α, μm	λ_β, μm	L, μm	$2r_y$, μm	δ_{cDHT}, μm	δx_{DHT}, μm	λ_{cm}, μm
A1	22	SHT/A: 900 °C/AC + aged	1158	…	…	…	…	…	…	2.7
A2	36	DHT/A: 1050 °C/900 °C AC + aged	1210	5.8	3.1	12.6	94	7.1	5.2	…
A3	41	DHT/A: 1125 °C/900 °C AC + aged	1161	8.2	2.6	15.3	132	9.6	7.5	…
A4	27	DHT/A: 1125 °C/900 °C OQ + aged	1254	5.7	3.6	13.2	49	3.9	2.0	…
	44	DHT/A/λ_v	1162	11.3	1.6	18.2	152	11.0	9.7	…
A5	25	DHT/A/λ_v	1259	2.5	4.8	10.3	42	3.3	1.9	…
B1	51	SHT/A: 950 °C/WQ + aged	1068	…	…	…	…	…	…	17.2
B2	62	DHT/A: 1050 °C/950 °C + aged	1020	5.4	7.3	25.6	392	26.6	23.4	…

Using a nominal value of 0.25 for σ/σ_{ys} in plane strain (from Ref 15) at $L/2r_y = 0.13$ gives:

$$\frac{\delta_{xDHT}}{\delta_{cDHT}} = 0.74 \text{ and } \delta_{xDHT} = 0.74 \times 7.1 \text{ μm or } 5.2 \text{ μm}$$

Thus, at a distance 12.6 μm ahead of the crack tip in the DHT/A microstructure, $\delta_{xDHT} = 5.2$ μm, compared with the transformed β matrix value of 2.7 μm for the SHT/A alloy. In theory, therefore, as $\delta_{xDHT} > \delta_{cm}$, the crack should cut through the α platelet. Thus, for alloy A2, Fig. 6(a) shows a crack propagating across α platelets at about 90° to the crack front.

Similar calculations for other toughness values for both alloy A and alloy B are shown in Table 2.

3.3 Analysis Based on Void Volume Fraction

A complementary analysis to the above can be obtained from the void volume fractions in the plastic zone ahead of the crack tips. Using Fullman's formula for void spacing, λ_v is equal to $(1 - f)/N_L$, where f is the volume fraction and N_L is the number of intercepts per unit length. From the quantitative analysis of the microstructural features, the λ_v spacing in alloy A ranged from 12 to 29 μm. From Fig. 2, these void fractions equate to the microstructural data shown in Table 2. Using the Hahn and Rosenfield (Ref 15) approach, Table 2 shows the relevant COD values.

From Table 2, for the 12 μm void spacing (K_{1c} = 44 MPa$\sqrt{m}$), and as $\delta_{xDHT} > \lambda_{cm}$, crack deflection would not be likely. The main crack in this case would be expected to cut through the platelets. In the case of the 32 μm void spacing, (K_{1c} = 25 MPa$\sqrt{m}$), $\delta_{xDHT} < \lambda_{cm}$, and the crack would be expected to deflect past the α platelet on average.

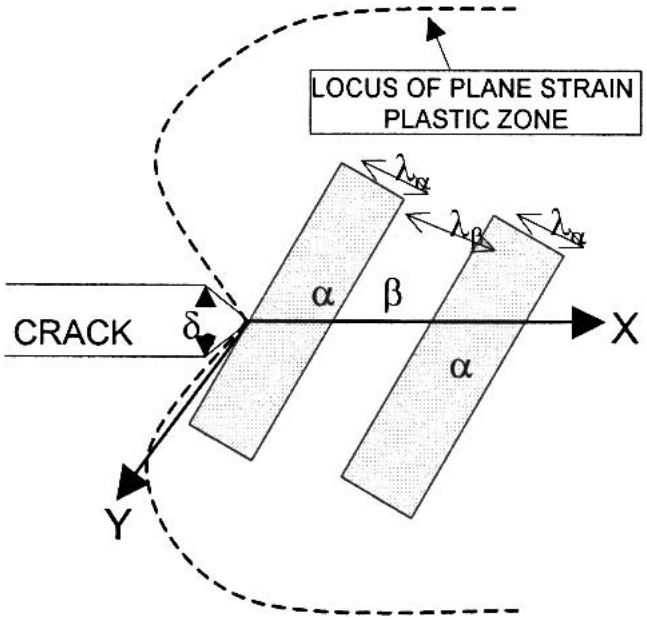

Fig. 5 Schematic of interaction of crack tip with a DHT/A microstructure

3.4 Potential for Crack Deflection: Alloy B

Similarly to alloy A, the above analysis can be extended to the tougher alloy B. Compilation of all the relevant microstructural data for alloy B is shown in Table 2 along with the relevant mechanical property data for the standard SHT/A condition and corresponding DHT/A condition.

For the DHT/A condition, the average λ_α and λ_β values are 5.4 and 7.3 μm, respectively. For alloy B, the microstructural unit that was used in Ref 10 was $\sqrt{2}(2\lambda_\alpha + \lambda_\beta)$ as a consequence of the increased toughness of this alloy relative to alloy A. Using the above values for λ_α and λ_β, $\sqrt{2}(2\lambda_\alpha + \lambda_\beta)$ is equal to 25.6 μm. The λ_{cm} value from the equation of Wells is 17.2 μm with the corresponding δx_{DHT} value equal to 23.4 μm. As $\delta_{xDHT} > \lambda_{cm}$, on average, the crack is likely to propagate across the platelets rather than deviate past them. Figure 1(d) shows several platelets being cut by the crack. Also shown is crack deviation past the platelets depending on local microstructural conditions. In both cases, however, increased energy is needed to either cut through the tougher α phase, or increase the crack path length, leading to higher fracture toughness values for the DHT/A alloys.

4. Discussion

In the SHT/A condition, the path of the crack is essentially perpendicular to the stress axis with the crack (Fig. 1a, b),

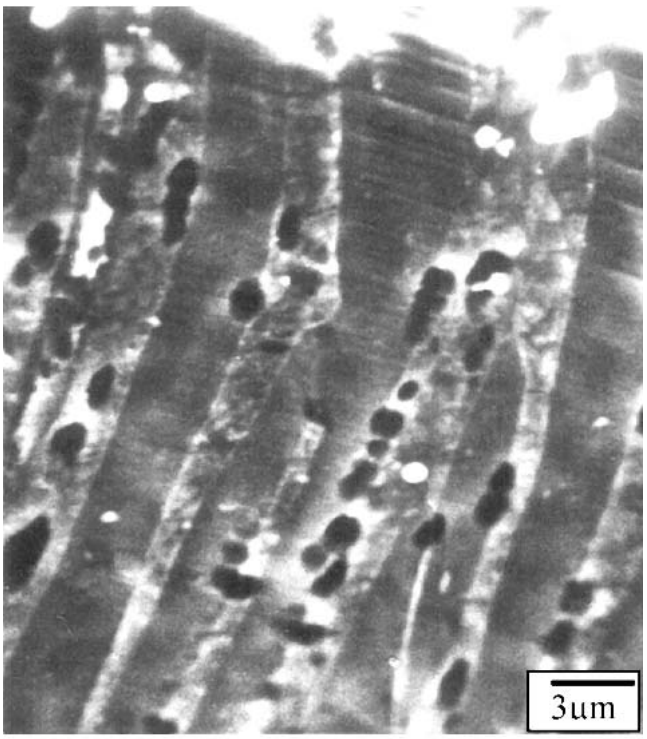

(a)

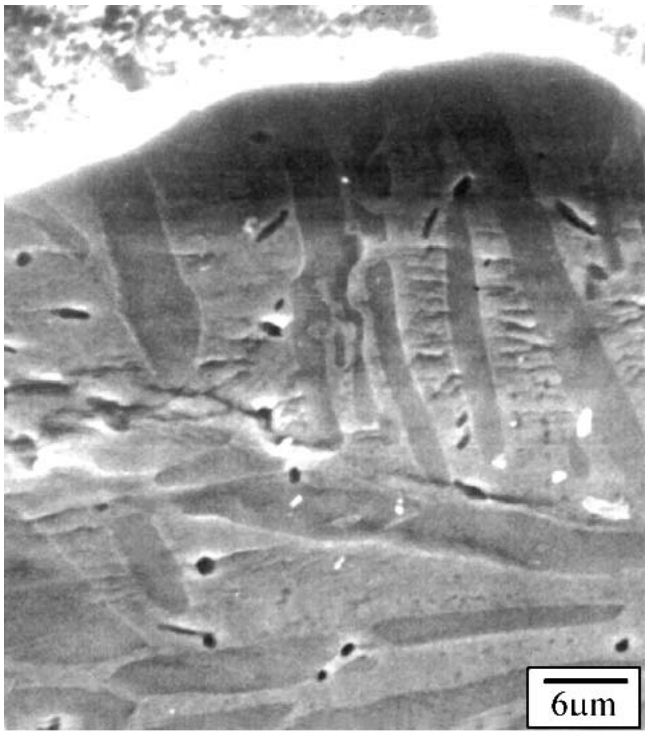

(b)

Fig. 6 Crack path through DHT/A microstructure: alloy A. (a) Crack propagating through α platelets in DHT structure. (b) Primary and secondary cracks in DHT

deviating only slightly in its path through the microstructure. On the other hand, a major consequence of the DHT/A (Fig. 1c, d) is a change in microstructure of both alloys from equiaxed morphology for the phases to an acicular structure, especially for the α phase. Consequently, the DHT/A microstructure consisted of alternate platelets of α, separated by the transformed β phase. A propagating crack, therefore, during fracture toughness testing would encounter a spectrum of α platelets at angles from 0 to 90° as it traversed the microstructure. Such an observation has been made by Margolin and Greenfield (Ref 8) and Gerberich and Baker (Ref 7). The consequence of the acicular α phase is, thus, to create an obstacle to the propagating crack, resulting in two options for further propagation depending on the energy level. In the first instance, when a crack meets an α platelet(s) it may deflect past the platelet, as in Fig. 1(c) and in part as in Fig. 1(d), or cut through the platelets, as in Fig. 6(a). The thickness of the platelet and the spacing between the platelets control the toughness and the path of the propagating crack through the microstructure. Widely spaced α platelets and thin platelets, as achieved by variations in the solution heat treatment temperatures, result in fracture toughness values of < 30 MPa$\sqrt{m}$. On the other hand, lower solution heat treatment temperatures result in thicker, more closely spaced platelets, leading to tougher microstructures, and consequently, more tortuous crack paths.

The reason that α platelet thickness is important (Fig. 4a, c) is that the α phase is tougher than the transformed β matrix, and thus, more energy is needed to cut through the α phase, especially if the aspect ratio of the platelets is large. Thus, if the δ_{xDHT} value ahead of the crack tip is not sufficiently high for the crack to propagate through the α platelet (a function of platelet thickness), then the path of least resistance is most likely via the α/β interface. On the other hand, if $\delta_{xDHT} > \lambda_{cm}$, then the COD ahead of the propagating crack will be sufficient for cutting through the α platelet. In addition, the spacing between the platelets also contributes to the toughness by constraining void growth between the platelets. Invariably, void formation occurs at the α/β interface (Fig. 6a), and a small λ_β value leads to increased toughness (Fig. 4b, d).

The above discussion is, however, only qualitative. The quantitative approach using the COD enables one to understand the contributions of the α platelet thickness and the interplatelet spacing. Previous research by Gerberich and Baker (Ref 7) and by Hahn and Rosenfield (Ref 15) has shown that if $\delta_{xDHT} < \lambda_{cm}$, then the crack will deviate past the α phase. If the opposite occurs, then the crack will cut through the platelet(s).

The data in Table 2 for alloy A reflects three situations where the COD values can be compared:

- The theory predicts the correct result.
- The theory fails.
- Values are too close to differentiate deviation or cutting of the α phase.

In the case of the first situation, theory predicts that $\delta_{xDHT} > \lambda_{cm}$, and this is corroborated by Fig. 6(a), which is a micrograph from alloy A2. Case 2 is typified by Fig. 1(c) in which, instead of cutting through the α platelets, the crack deviates in a tortuous manner past them. This apparent failure of the theory is related to the path of least resistance through the microstructure. In this case, the aspect ratio of the platelets locally is low, and thus, the crack spends less energy deviating past the platelets rather than using more energy to cut through them. The final example is case 3 in which both COD values are close and low. In this case, the local microstructure (e.g., Fig. 6b) shows the crack cutting α platelets, but a subcrack propagates between a colony of vertically oriented platelets and others perpendicular to the main crack.

For alloy B, theory predicts cutting of the α platelets as $\delta_{xDHT} > \lambda_{cm}$. Figure 1(b), however, shows both cutting and deviating occurring depending on the local microstructure and energy minimization requirements. The crack traveling from the top to the bottom of the micrograph initially deviates along the α/transformed β interface. It then cuts back across platelets at 90° before returning to the main axis of cracking.

A final comment is needed relative to the results. It is not proposed that the Hahn and Rosenfield (Ref 15)/Goodier and Field (Ref 12) theory and the equations used in the article are highly accurate. The size of the plastic zone, for example, is not easily evaluated and depends on the degree of work hardening and the actual stress conditions, as well as the effects of crack blunting. The theory is, however, useful in comparing crack behavior. From the results, it can be seen that by comparing the SHT/A COD values with the DHT/A values, that reasonable assumptions about how and why the crack takes a particular path are reasonably predictable. Qualitatively, one can see that the α platelet size and morphology can be rationalized relative to its role, as well as its spacing relative to crack propagation, and the role of the DHT/A microstructure in increasing fracture toughness in Ti alloys.

5. Conclusions

An investigation of the COD predictions ahead of a crack in SHT/A microstructure of two Ti alloys relative to the DHT/A microstructure has shown:

- The DHT/A produces a microstructure with α platelets in a transformed β matrix.
- The SHT/A microstructure, on the other hand, consists of equiaxed α in a transformed β matrix.
- Due to the DHT/A microstructure, crack propagation occurs either by deflecting past suitably oriented α platelets, or by cutting through them.
- In both cases, energy is expended, either in deviating past the α platelets or cutting through them.
- COD predictions based on an analysis of the Hahn and Rosenfield (Ref 15) and Goodier and Field (Ref 12) approaches is quantitatively capable of differentiating the relative cracking behavior of microstructures having various fracture toughness levels.
- The reasons for the theory not being able to predict correct cracking behavior are related to the aspect ratio of the α platelets in a three-dimensional microstructure.

References

1. J.E. Coyne, The Beta Forging of Titanium Alloys, *The Science, Technology & Application of Titanium,* R.I. Jaffee and N.E. Promisel, Ed., Pergamon Press, 1968, p 97-110

2. F.C. Holden, H.R. Ogden, and R.I. Jaffee, Heat Treatment & Mechanical Properties of Ti-Mo Alloys, *J. Met.,* Vol 8, 1956, p 1388-1393
3. F.C. Holden, H.R. Ogden, and R.I. Jaffee, Heat Treatment, Structure and Mechanical Properties of Ti-Mn Alloys, *Trans. Am. Inst. Min. Metall. Pet. Eng.,* Vol 200, 1954, p 169-184
4. A.W. Goldenstein and W.A. Rostocker, Relationship between Heat Treatment, Structure & Mechanical Properties of a Titanium Alloy Containing 4% Cr and 2% Mo, *Trans. Am. Soc. Met.,* Vol 49, 1957, p 315-323
5. M.A. Greenfield, P.A. Farrar, and H. Margolin, Thermo-Mechanical Strengthening of High Strength Titanium Alloys, *The Science, Technology and Application of Titanium,* N. Promisel and R.I. Jaffee, Ed., Pergamon Press, 1970, p 795-808
6. W.P. Fentiman, R.E. Goosey, R.J.T. Hubbard, and M.D. Smith, Exploitation of a Simple Alpha Titanium Alloy Base in the Development of Alloys of Diverse Mechanical Properties, *The Science, Technology and Application of Titanium,* N. Promisel and R.I. Jaffee, Ed., Pergamon Press, 1970, p 987-999
7. W.W. Gerberich and G.S. Baker, Toughness of Two-Phase 6Al-4V Titanium Microstructures, *Applications Related Phenomena in Titanium Alloys,* STP 432, ASTM, 1967, p 80-99
8. H. Margolin and M.A. Greenfield, The Interrelationship of Fracture Toughness & Microstructure in a Ti/5.2Al/5.5V/0.9Fe/0.5Cu Alloy, *Metall. Trans.,* Vol 2, 1971, p 841-847
9. D. Eylon, J.A. Hall, C.M. Pierce, and D.L. Ruckle, Microstructure & Mechanical Properties Relationships in the Ti-11 Alloy at Room & Elevated Temperature, *Metall. Trans.,* Vol 7, 1976, p 1817-1826
10. N.L. Richards, Quantitative Evaluation of Fracture Toughness—Microstructural Relationships in Alpha-Beta Titanium Alloys, *J. Mater. Eng. Perform.,* Vol 13 (No 2), April 2004, p 218-225
11. T.E. Green and C.D. Minton, The Effect of Beta processing on Properties of Titanium Alloys, *The Science, Technology and Application of Titanium,* N. Promisel and R.I. Jaffee, Ed., Pergamon Press, 1970, p 111-119
12. J.N. Goodier and F.A. Field, Plastic Energy Dissipation in Crack Propagation, *Fracture of Solids,* D.C. Drucker and J.J. Gilman, Ed., 1963, Interscience, p 103-118
13. A.A. Wells, Application of Fracture Mechanics At and Beyond General Yielding, *Br. Weld. J.,* Vol 10, 1963, p 563-570
14. J.R. Rice, Mathematical Analysis of Fracture in the Mechanics of Fracture, *Fracture: An Advanced Treatise,* H. Leibovitz, Ed., Academic Press, Vol II, 1968, p 191-311
15. G.T. Hahn and A.R. Rosenfield, Plastic Energy Dissipation in Crack Propagation, *Acta Metall.,* Vol 13, 1965, p 293-306
16. G.R. Irwin, Analysis of Stresses and Strains Near the End of a Crack Traversing a Plate, *J. Appl. Mech.,* Vol 24, 1957, p 361-364